

Study of the Mach-Zehnder Interferometric Technique for Dielectric Resonator Tuning

Héctor J. De Los Santos¹, Christian Rusch², Yi Chen³

¹NanoMEMS Research, LLC, Irvine, CA 92623 USA, ²Karlsruher Institut für Technologie, Institut für Hochfrequenztechnik und Elektronik 76131 Karlsruhe, Germany, ³Christian-Albrechts-Universität zu Kiel 24143 Kiel, Germany

Abstract — The modulation of a metallic microwave-scale Mach-Zehnder interferometer (MZI) coupled to a dielectric resonator (DR) may be used to tune the resonance frequency of the latter. In this paper, we report on a theoretical study to develop an understanding of the intrinsic tuning properties of an MZI Ring-DR-Microstrip line system and, for the first time, present an experimental verification of the concept.

Index Terms — Dielectric Resonator, Tuning, Satellite Communications, Mach-Zehnder Interferometer, Microwaves.

I. INTRODUCTION

Rings and ring-based components, such as, resonators and filters, have been extensively studied. Little work has been done, however, on applying rings as *agents to effect the tuning* of dielectric resonators (DR). In this novel context, it is conceptually profitable to think of the ring as operating as a Mach-Zehnder interferometer (MZI), and to explore how, when coupled to a DR, modulation of one of the MZI paths causes tuning of the DR. This approach is believed to be important because it paves the way to high-Q-preserving DR tuning. This paper presents a theoretical study of the intrinsic tuning properties of a metallic microwave-scale MZI-DR-transmission line system, of the type employed in DR oscillators, together with, for the first time, experimental verification of the concept. Section II presents an overview of the MZI ring and motivates its utilization as a *tuning agent* for DRs. Section III introduces the MZI-DR-Microstrip line system and presents the experimental verification of DR tuning using this scheme.

II. MZI-BASED TUNING CONCEPT

A. Overview of the Mach-Zehnder Interferometer

The MZI, in its implementation as a metallic microstrip ring, is depicted in Fig. 1. It consists of two parallel curved paths, $i=1, 2$, forming an annular ring, characterized by propagation constant $k_i = \omega \sqrt{L_r C_r}$, where ω is the wave frequency and L_r and C_r the inductance and capacitance per unit length. When the propagation constants are equal, the input wave, after

being split at the input junction, propagates down both paths and is recreated at the output junction, where recombination occurs. On the other hand, causing the propagation constants

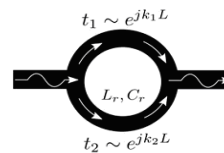


Fig. 1. Sketch of Mach-Zehnder Interferometer.

of the two ring paths to be unequal results in a wave amplitude at the output that exhibits a degree of interference. Assuming unit input wave amplitude and equal splitting in both ring arms, Fig. 1, the output wave amplitude is $t = e^{ik_1L} / \sqrt{2} + e^{ik_2L} / \sqrt{2}$. Then, the interference behavior is mathematically captured by the transmission coefficient of the structure, namely:

$$T = |t|^2 = 1 + \cos[L \cdot (k_2 - k_1)], \quad (1)$$

where L is half the ring mean circumference. Clearly, the maximum of T is obtained whenever the cosine argument equals zero or an integer multiple of 2π . Now, if the MZI ring had no outgoing transmission line, it is easy to see that there could be no transmission and, therefore, the waves on each ring arm would counter propagate, establishing a standing wave pattern in the ring. Under these circumstances, it is well known that a resonance condition exists, whose frequency is well approximated by:

$$f_n = \frac{nc}{2L \sqrt{\epsilon_{eff}(f)}}, \quad (2)$$

where $n=1, 2, \dots$, is the mode number, c is the speed of light in vacuum, and $\epsilon_{eff}(f)$ is the frequency-dependent relative dielectric constant of the substrate supporting the ring.

B. MZI Ring Tuning

To study the *intrinsic* tuning properties of the *tunable* ring, the structure shown in Fig. 2 is considered. It may be construed as consisting of an asymmetric ring made up of the parallel connection of one microstrip transmission line (TL) of

length L_4 and width w , and another TL consisting of the tandem connection of three TL segments of length and widths (L_1, w) , (L_2, w_2) , (L_3, w) , respectively. Other asymmetric MZI ring parameters are its mean radius, r , and the mean circumference, $2L = 2\pi r = L_1 + L_2 + L_3 + L_4$, with:

$$L_1 = r \left(\pi - \left[\frac{\theta}{2} + \phi \right] \right), \quad (3)$$

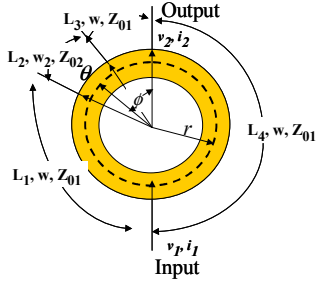


Fig. 2. Description of asymmetric microstrip MZI ring: θ : Tuning Sector; ϕ : Azimuthal position of tuning sector; r : mean radius; w : Unloaded ring width; w_2 : Tuning sector (loaded) ring width; Z_{01} , Z_{02} : characteristic impedances of indicated segments.

$$L_2 = r\theta, \quad (4)$$

$$L_3 = r \left(\phi - \frac{\theta}{2} \right), \quad (5)$$

$$L_4 = r\pi. \quad (6)$$

For a given mean ring circumference, $2L$, tuning is effected by changing (L_2, w_2) . This segment is positioned at the azimuthal angle ϕ , and has an angular extent θ , Fig. 2.

Additionally, at a frequency f , the electrical parameters of the ring are given by the propagation constant of each TL segment j , $\gamma_j = \alpha_j + i\beta_j = \alpha_j + ifn_j$, where α_j and β_j are the attenuation and phase constants in segment j , with $\beta_j = 2\pi f \sqrt{\mu_0 \epsilon_0 \epsilon_{eff_j}} = fn_j$, and μ_0 and ϵ_0 are the vacuum permeability and permittivity, respectively. The intrinsic tuning properties of the asymmetric ring are obtained by conceptually assuming it to be a two-port network, driven at its input and output ports by voltages and currents v_1, i_1 and v_2, i_2 , respectively, Fig. 2. The ring's return loss, $S_{R_{11}} = S_{R_{11N}}/S_{R_D}$, and transmission, $S_{R_{21}} = S_{R_{21N}}/S_{R_D}$, were obtained analytically in terms of the overall ring admittance parameters $(Y_{R_{ij}})$, by computing the ABCD parameters of the two paths, converting the parameters of each path to admittance parameters, and adding the resulting Y-parameters of each path. The S-parameter expressions are long, so their numerators, $S_{R_{11N}}$ and $S_{R_{21N}}$, and their common denominator, S_{R_D} are given separately in Eq. (7), where Z_0 is the reference impedance and the

attenuation (α) has been taken as zero. To the best of the authors' knowledge, these expressions are not available in the literature. The S-parameters, computed with Eqs.(7), are plotted in Fig. 3(a); the transmission follows the same behavior of the symmetric ring (Eq. 1). There are no closed-form expressions for the resonance frequencies of the asymmetric MZI ring, since they derive from the transcendental equation obtained from seeking the roots of Eq. (10c), however, in a design, Eq. (2) is a good starting point.

The formulas are verified by comparing their predicted tuning frequencies, given by the minimum of $S_{R_{11}}$ as computed from Eqs. (10), with the frequency of the minima obtained from CST [1] simulations, Fig. 3(b). As clearly seen in Fig. 3(c), increasing the tuning sector length, θ , causes the resonance frequency to decrease, as should correspond to adding the tuning sector capacitance. It must be mentioned also, that given the nonlinear dependence of Eqs. (10) on ϕ (through L_1 and L_3), the tuning range is a function of the azimuthal angle ϕ .

C. MZI Ring Coupling to Transmission Line

While the properties of ring-TL coupling have been studied, studies on the effect that ring tuning, as revealed here, produces on TL properties are lacking. Simulations in CST, Fig. 3(d), exhibit a minimum in the transmission, whose frequency decreases with increase in tuning sector angle. This suggests a way of tuning the transmission of the microstrip line and, as shown next, may be exploited to tune a DR.

III. MZI-BASED DIELECTRIC RESONATOR TUNING CONCEPT AND EXPERIMENTAL VERIFICATION

The idea of applying the tuned MZI ring to effect DR tuning derives from extending the DR-microstrip model [2], Fig. 4, to the DR-MZI ring, except that in the latter case the transformer coupling [2] N_i becomes *variable*, Fig. 5, reflecting MZI tuning. This tuning, in turn, changes the impedance "seen" by the DR and causes its resonance frequency to change. The study conducted, to be described in detail at the conference, led to an optimized topology with greater MZI-DR-TL coupling, namely, one in which the ring was deformed. This structure was fabricated and tested. In particular, the variation in tuning sector angles was realized by fabricating three separate structures, Fig. 6. Defining the tuning sector this way in the study provides a controlled way (i.e., one that is reproducible by others) of varying its size, which otherwise could be done by, e.g., manually placing on the ring gold ribbons of varying sizes, as is customary practice when "tuning" microwave integrated (i.e., Alumina-based, etc.) circuits. The measured S_{21} and S_{11} for these structures, shown in Fig. 6(c), (d), exhibit a tuning range of

$$S_{R_{-11-N}} = 0.5 \csc[fL_4 n_1] \left(-8Z_0^2 Z_{01} Z_{02} + 2Z_{01} Z_{02} (Z_{01}^2 \cos[f(L_1 + L_3 - L_4)n_1] + (4Z_0^2 - Z_{01}^2) \cos[f(L_1 + L_3 + L_4)n_1]) \cos[fL_2 n_2] \right) -$$

$$(Z_{01}(-2iZ_0(Z_{01} - Z_{02})(Z_{01} + Z_{02}) \cos[f(L_1 - L_3 - L_4)n_1] + 2iZ_0(Z_{01} - Z_{02})(Z_{01} + Z_{02}) \cos[f(L_1 - L_3 + L_4)n_1]) +$$

$$Z_{01}(-Z_{01}^2 + Z_{02}^2) \sin[f(L_1 - L_3 - L_4)n_1] + Z_{01}(Z_{01}^2 + Z_{02}^2) \sin[f(L_1 + L_3 - L_4)n_1] + Z_{01}(Z_{01} - Z_{02})(Z_{01} + Z_{02}) \sin[f(L_1 - L_3 + L_4)n_1] +$$

$$(4Z_0^2 - Z_{01}^2)(Z_{01}^2 + Z_{02}^2) \sin[f(L_1 + L_3 + L_4)n_1] \sin[fL_2 n_2]) \quad (7a)$$

$$S_{R_{-21-N}} = -4iZ_0 Z_{01} (Z_{01} Z_{02} + \csc[fL_4 n_1] (Z_{01} Z_{02} \cos[fL_2 n_2] \sin[f(L_1 + L_3)n_1] + (Z_{02}^2 \cos[fL_1 n_1] \cos[fL_3 n_1] - Z_{01}^2 \sin[fL_1 n_1] \sin[fL_3 n_1]) \sin[fL_2 n_2])) \quad (7b)$$

$$S_{R_{-D}} = Z_{01} Z_{02} \csc[fL_4 n_1] (4Z_0^2 + \cos[fL_2 n_2] (Z_{01}^2 \cos[f(L_1 + L_3 - L_4)n_1] - (4Z_0^2 + Z_{01}^2) \cos[f(L_1 + L_3 + L_4)n_1] - 4iZ_0 Z_{01} \sin[f(L_1 + L_3 + L_4)n_1])) +$$

$$2(\cos[fL_3 n_1] (\cos[fL_1 n_1] (Z_0^2 Z_{01}^2 + (Z_0^2 + Z_{01}^2) Z_{02}^2 - 2iZ_0 Z_{01} Z_{02} \cot[fL_4 n_1] + Z_0 (Z_{01}^2 + Z_{02}^2) (iZ_{01} + Z_0 \cot[fL_4 n_1]) \sin[fL_1 n_1]) +$$

$$(Z_0 (Z_{01}^2 + Z_{02}^2) \cos[fL_1 n_1] (iZ_{01} + Z_0 \cot[fL_4 n_1]) - (Z_0^4 + Z_0^2 (Z_{01}^2 + Z_{02}^2) - 2iZ_0 Z_{01}^3 \cot[fL_4 n_1]) \sin[fL_1 n_1] \sin[fL_3 n_1]) \sin[fL_2 n_2]) \quad (7c)$$

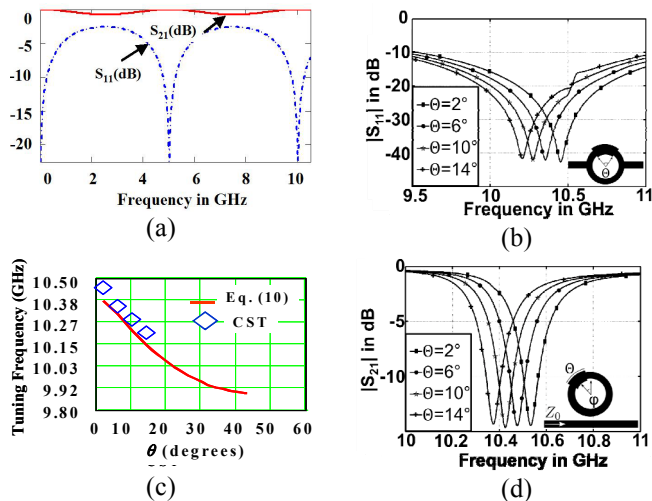


Fig. 3. (a) S-parameters of asymmetric MZI ring at $\phi=90^\circ$, $\theta=4^\circ$. (b) Insertion Loss of CST-simulated loaded MZI ring (sketch in inset), with $\phi=90^\circ$, for various tuning sector angles. (c) Tuning frequency versus tuning angle for MZI ring in Fig. 3(b). MZI ring parameters: mean ring diameter, 6.95 mm; ring trace width, 0.5 mm; substrate thickness and relative permittivity, 0.635 mm and 10.2, respectively; metallization thickness, 0.017 mm. The tuned-sector width is 1 mm. (d) CST-computed microstrip transmission (S_{21}) versus frequency with tuned-sector angle, θ , as a parameter, and $\phi=135^\circ$. The tuned sector width is 1 mm.

32 MHz and a Q factor between 983 to 1089, for sector angles $\theta=2^\circ, 6^\circ, 10^\circ$, thus verifying the DR tuning concept.

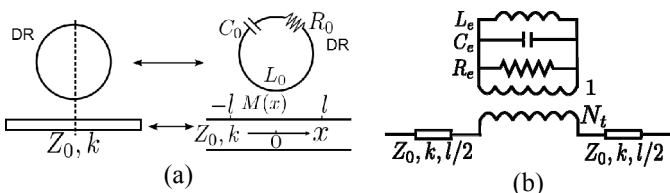


Fig. 4. (a) Distributed DR-Microstrip model; (b) Lumped DR-Microstrip circuit model.

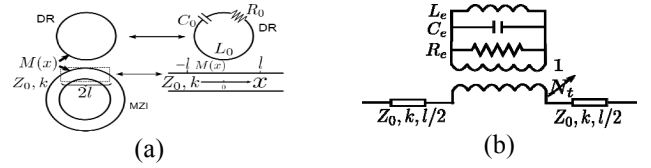


Fig. 5. (a) DR-MZI ring distributed model; (b) Lumped DR-MZI ring circuit model.

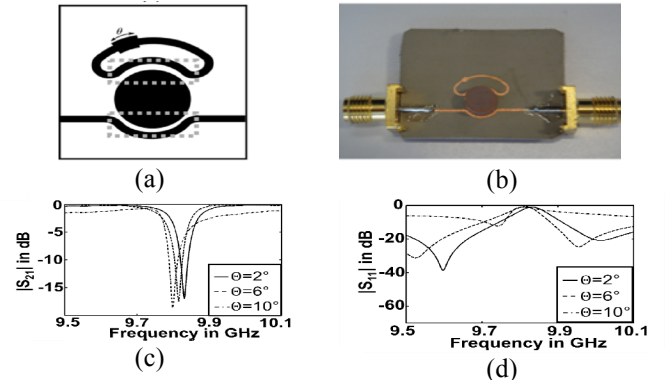


Fig. 6. (a) MZI Ring-DR-Microstrip structure sketch (in practice, the indicated tuning sector may be implemented manually with a gold ribbon, until the desired resonance frequency is obtained); (b) Picture of typical fabricated MZI Ring-DR-Microstrip structure. Three structures with $\theta=2^\circ, 6^\circ, 10^\circ$ were fabricated; (c), (d) Measured S_{21} and S_{11} of fabricated structure shown in (b). The nominal DR Q specified by the manufacturer was 5000.

ACKNOWLEDGEMENT

Work supported by a German Research Foundation (DFG) Mercator Visiting Professorship award to H.J. De Los Santos.

REFERENCES

- [1] Computer Simulation Technology, Inc, CST Studio Suite 2010.
- [2] Y. Komatsu and Y. Murakami, "Coupling coefficient between microstrip line and dielectric resonator," *IEEE Trans. Microwave Theory & Tech.*, vol. 31, pp. 34-40, 1983.